Full protection against all four SARS-CoV-2 variants of concern (VOC) in hamsters requires revision of spike antigen used for vaccination.

Sapna Sharma [a], Thomas Vercruysse [a, b], Lorena Sanchez-Felipe [a], Winnie Kerstens [a, b], Rana Abdelnabi [a], Caroline Foo [a], Viktor Lemmens [a], Dominique Van Looveren [a, b], Piet Maes [c], Guy Baele [d], Birgit Weynand [e], Philippe Lemey [d], Johan Neyts [a], Hendrik Jan Thibaut [a, b, &], and Kai Dallmeier [a, &, #]

[a] KU Leuven Department of Microbiology, Immunology and Transplantation, Rega Institute, Laboratory of Virology, Molecular Vaccinology and Vaccine Discovery, Leuven, Belgium.

[b] KU Leuven Department of Microbiology, Immunology and Transplantation, Rega Institute, Laboratory of Virology and Chemotherapy, Translational Platform Virology and Chemotherapy, Leuven, Belgium.

[c] KU Leuven Department of Microbiology, Immunology and Transplantation, Rega Institute, Laboratory of Clinical and Epidemiological Virology, Zoonotic Infectious Diseases Unit, Leuven, Belgium.

[d] KU Leuven Department of Microbiology, Immunology and Transplantation, Rega Institute, Laboratory of Clinical and Epidemiological Virology, Evolutionary and Computational Virology, Leuven, Belgium.

[e] KU Leuven Department of Imaging and Pathology, Translational Cell and Tissue Research, B-3000 Leuven, Belgium.

& contributed equally

correspondence should be addressed to: kai.dallmeier@kuleuven.be

Abstract

Current licensed COVID-19 vaccines are based on antigen sequences of initial SARS-CoV-2 isolates that emerged in 2019. By mid 2021 these historical virus strains have been completely replaced by new cosmopolitan SARS-CoV-2 lineages. The ongoing pandemic has been further driven by emerging variants of concern (VOC) Alpha, Beta, Gamma and, lately predominant, Delta. These are characterized by an increased transmissibility and possible escape from naturally acquired or vaccine-induced immunity. We here show, using a YF17D-vectored first-generation COVID-19 vaccine (Sanchez-Felipe et al., 2021) and a stringent hamster challenge model (Abdelnabi et al., 2021) that the immunity elicited by a prototypic spike antigen is insufficient to provide optimal protection against the Beta VoC, urging for an antigenic update. We therefore designed an updated second-generation vaccine candidate that carries the sequence of a spike antigen that includes crucial epitopes from multiple VOCs. This vaccine

candidate yielded a marked change in target antigen spectrum covered as demonstrated by (*i*) antigenic cartography and (*ii*) full protection against infection and virus-induced disease caused by any of the four VOCs (Alpha, Beta, Gamma and Delta) used for challenge. This more universal COVID-19 vaccine candidate also efficiently blocked direct transmission of VOC Delta from vaccinated infected hamsters to non-vaccinated sentinels under prolonged co-housing conditions. In conclusion, our data suggest that current first-generation COVID-19 vaccines need to be adapted to cover emerging sequence diversity of VOC to preserve vaccine efficacy and to contain virus spread at the community level.

Key Words: SARS-CoV-2, variants of concern (VOC), vaccine efficacy, antigenic cartography, virus transmission, hamster model

Introduction

Severe Acute Respiratory Syndrome Corona Virus 2 (SARS-CoV-2) emerged as zoonosis likely from a limited number of spill-over events into the human population (Holmes et al., 2021). Nevertheless, the ongoing COVID-19 pandemic is entirely driven by variants that evolved during subsequent large-scale human-to-human transmission. In particular, mutations within the viral spike protein are under continuous surveillance (ECDC, 2021) considering their role in viral pathogenesis and as target for virus-neutralizing antibodies (nAb). Following early diversification, the D614G SARS-CoV-2 variant (B.1 lineage) became dominant in March 2020. Consecutively, Variants of Concern (VOC) were identified in many countries with increased transmissibility, virulence and evidence for escape from naturally acquired and vaccine-induced immunity (Tian et al., 2021). Each of the four currently recognized VOCs harbor a unique set of partially convergent, partially unique spike mutations as compared to prototypic (Wuhan) or early European D614G (B.1) lineages of SARS-CoV-2, namely VOC Alpha (B.1.1.7; N501Y D614G), Beta (B.1.351; K417N E484K N501Y D614G), Gamma (P.1; K417T E484K N501Y D614G) and Delta (B.1.617.2; K417T L452R T478K D614G P681R)(Cella et al., 2021). N501Y first detected in VOC Alpha has been linked to an enhanced transmissibility due to an increased affinity for the human ACE-2 receptor (Liu et al., 2021a; Moyo-Gwete et al., 2021). Subsequent emergence of E484K within this lineage hampers the activity of nAb suggestive for immune escape (Graham et al., 2021; Muik et al., 2021; Wu et al., 2021). Likewise, a combination of K417N E484K (Greaney et al., 2021) may explain a marked reduction in vaccine efficacy (VE) of some vaccines such as ChAdOx1 nCoV-19 (AstraZeneca, Vaxzevria) in clinical trials in South Africa during high prevalence of VOC Beta (Madhi et al., 2021). Similarly, sera from vaccinees immunized with first-generation mRNA (Pfizer-BioNTech, Cormirnaty; Moderna, mRNA-1273) or nanoparticle subunit vaccines (Novavax) showed a substantial drop in neutralizing capacity for VOC Beta (Wang et al., 2021). Furthermore VOC Gamma harboring K417T E484K emerged in regions of Brazil with high seroprevalence, hence despite naturally acquired immunity against prototypic SARS-CoV-2 (Sabino et al., 2021). VOC Delta was first identified in October 2020 in India (Cherian et al., 2021; Hoffmann et al., 2021; Yadav et al., 2021) and has since then become the predominant SARS-CoV-2 lineage worldwide, driven by a substantially increased transmissibility (Liu et al., 2021b).

All currently licensed COVID-19 vaccines and vaccine candidates in advanced clinical development are based on antigen sequences of early SARS-CoV-2 isolates that emerged in 2019 (Kyriakidis et al., 2021). We also reported on a YF17D-vectored SARS-CoV-2 vaccine candidate using prototypic spike as vaccine antigen (YF-S0; S0) that had an outstanding preclinical efficacy against homologous challenge (Sanchez-Felipe et al., 2021). However, we now demonstrate to what extent VE of S0 and hence first-generation spike vaccines in general, may decline when trialed against VOC Beta in a stringent hamster model (Abdelnabi et al., 2021). Therefore, a second-generation vaccine candidate (YF-S0*) was designed by (*i*) modifying its antigen sequence to catch up with the evolving spike variant

83 spectrum, in combination with (*ii*) a further stabilized protein conformation (Juraszek et al., 2021).
84 Furthermore, we here demonstrate that this new S0* vaccine candidate provides full protection against
85 all current VOCs (Alpha, Beta, Gamma and Delta). Finally, hamsters vaccinated with S0* do no longer
86 transmit the virus to non-vaccinated sentinels during close contact, even under conditions of prolonged
87 co-housing and exposure to a high infectious dose of VOC Delta.

88 Our findings suggest that first-generation COVID-19 vaccines may need to be adapted to follow the
89 evolution of SARS-CoV-2 variants fueling the ongoing pandemic. This is important as new variants
90 may emerge that contain critical combinations of driver mutations responsible for both nAb escape (e.g.,
91 E484K) (Greaney et al., 2021) and enhanced transmission (e.g., N501Y; P681R/H) (Collier et al., 2021)
92 already observed in variant of interest (VOI) Mu (B.1.621) currently in surge in some regions of Latin
93 America (ECDC, 2021).
94

95 **Results and Discussion**

96 **Reduced efficacy of first-generation spike vaccine against VOCs Alpha and Beta**

97 To assess VE of prototypic spike antigen against VOCs, hamsters were vaccinated twice with each 10^4
98 PFU of YF-S0 (S0) or sham at day 0 and 7 via the intraperitoneal route (Sanchez-Felipe et al., 2021)
99 (**Fig. 1A**). Serological analysis at day 21 confirmed that 30/32 (94%) vaccinated hamsters had
100 seroconverted to high levels of nAbs against prototypic SARS-CoV-2 with geometric mean titre (GMT)
101 of 2.3 $\log_{10}$ (95% CI 2.0-2.6) (**Fig. 1B**). Next, animals were challenged intranasally with $1x10^3$ $TCID_{50}$
102 of either prototypic SARS-CoV-2, VOC Alpha or Beta as established and characterized before in the
103 hamster model (Abdelnabi et al., 2021). At day four after infection (4 dpi), viral replication was
104 determined in lung tissue by qPCR and virus titration (**Fig. 1C, D**). In line with what was originally
105 described for S0 (Sanchez-Felipe et al., 2021), a marked reduction in viral RNA and infectious virus
106 loads down to undetectable levels (up to $6\log_{10}$ reduction) was observed in the majority of animals
107 challenged with either prototypic SARS-CoV-2 (8/10; 86% VE) or VOC Alpha (9/10; 88% VE). In
108 those animals (2/10 and 1/10, respectively) that were not completely protected, virus loads were at least
109 100 times lower than in infected sham controls. By contrast and despite full immunization, S0
110 vaccination proved to be less effective against VOC Beta, with only 4/12 hamsters without detectable
111 infectious virus (60% VE). Nonetheless, in the remaining 8/12 animals with breakthrough infection by
112 VOC Beta, viral replication was tempered as vaccination still resulted in a 10 to 100-fold reduction in
113 infectious virus titres relative to sham.

114 Logistic regression used to define immune correlates of protection (van der Lubbe et al., 2021)
115 confirmed that comparable nAb levels were required for protection against prototypic SARS-CoV-2
116 (1.5 $\log_{10}$ for 50% and 2.9 $\log_{10}$ for 90% protection) and VOC Alpha (1.2 $\log_{10}$ for 50% and 2.5 $\log_{10}$ for
117 90% protection) (**Fig. 1E**). Intriguingly, for VOC Beta a markedly (up to 25x) higher nAb threshold (2.6
118 $\log_{10}$) was required for 50% protection. Importantly, no 90% protective nAb threshold could be defined
119 anymore for VOC Beta infection, considering the high number of S0 vaccinated animals with viral
120 breakthrough ($>10^2$ $TCID_{50}$/100mg lung tissue) (van der Lubbe et al., 2021). Overall, these data suggest
121 that first-generation vaccines employing prototypic spike as antigen may generally suffer from a
122 markedly reduced efficacy against emerging SARS-CoV-2 variants, such as VOC Beta.

123 **Updated spike antigen offers complete protection against full range of VOCs**

124 Although prototype S0 showed induction of high titres of nAb against prototypic SARS-CoV-2 (**Fig.**
125 **1B**) and protective immunity against prototypic SARS-CoV-2 and VOC Alpha (**Fig. 1C-E**), the
126 prototypic spike antigen failed to induce consistent nAb responses against remaining VOCs (**Fig. 2A**).
127 Most importantly, YF-S0 vaccination resulted only in poor seroconversion and low nAb titres against
128 VOC Beta (seroconversion rate 15/32; GMT 1.0 $\log_{10}$, 95% CI of 0.6-1.3;) and Gamma (19/32; GMT

129 1.3 $\log_{10}$, 95% CI 0.9-1.8). Intriguingly, also a pool of human convalescent serum used as benchmark
130 (WHO standard NIBSC 20/130) originating from 2020 prior to the surge of VOC (**Fig. 2A-B**) showed
131 a similar loss of activity against VOC Beta, in line with what was observed in our hamster sera (**Fig.**
132 **2A**).

133 It is not clear if the full spectrum of antigenic variability of current VOCs and emerging variants can be
134 covered by a COVID-19 vaccine that is based on a single antigen (Lopez Bernal et al., 2021; Rubin,
135 2021). In an attempt to generate a more universal SARS-CoV-2 vaccine (YF-S0*, S0*), we adapted the
136 spike sequence in our original YF-S0 construct to include the full amino acid spectrum from VOC
137 Gamma, plus three extra proline residues (A892P, A942P and V987P) to stabilize spike in conformation
138 favorable for immunogenicity (Hsieh et al., 2020; Juraszek et al., 2021) (**Fig. 2C**). YF-S0* proved to be
139 highly immunogenic against prototypic SARS-CoV-2, with nAb levels reaching GMT of 2.2 $\log_{10}$ (95%
140 CI 1.8-2.6) and a seroconversion rate of 21/24 (**Fig. 2D**), comparable to original YF-S0 (GMT 2.3 $\log_{10}$,
141 95% CI 2.0-2.6; 30/32 seroconversion rate) (**Fig. 2A**). Also, for both constructs, seroconversion rates
142 and nAb levels against VOC Delta were similar (YF-S0: 30/32; GMT 2.0 $\log_{10}$, 95% CI 1.7-2.2; YF-
143 S0*: 22/24; GMT 2.0 $\log_{10}$, 95% CI 1.6-2.3). Notably, for YF-S0*, nAb levels and seroconversion rates
144 against VOC Beta (GMT 2.9 $\log_{10}$, 95% CI 2.6-3.2; seroconversion rate 23/24) and Gamma (GMT 3.0
145 $\log_{10}$, 95% CI 2.8-3.2; seroconversion rate 24/24) were markedly increased (by 50 to 80-fold for GMT;
146 1.7 to 2-times more frequent seroconversion) (**Fig. 2A, D**).

147 We further studied the pattern of cross-reactivity of the sera raised by the original (YF-S0) and updated
148 (YF-S0*) vaccine antigen against four different virus variants (prototype; VOCs Beta, Gamma and
149 Delta) using antigenic cartography (Smith et al., 2004). VOC Alpha was not considered since it did not
150 differ from the prototype virus, neither regarding VE of S0 nor nAb titre as correlate protection (**Fig. 1**).
151 Specifically, we constructed a two-dimensional projection that geometrically maps median serum
152 neutralization titres (SNT_{50}) between sera and respective antigens as antigenic distances. This revealed
153 a pattern of antigenic diversification between prototype virus on the one hand and VOCs Beta and
154 Gamma on the other hand, with VOC Delta being mapped closer to the prototype virus as compared to
155 Beta and Gamma. This is consistent with recently described patterns of convergent evolution in spike
156 for VOCs Beta and Gamma, and Delta climbing a different fitness peak (Martin et al., 2021). In line
157 with the visual pattern of clustering, antigenic distances for S0* sera were significantly larger to
158 prototype and VOC Delta as compared to Beta and Gamma (t-test; $p<0.001$). Intriguingly, this obvious
159 antigenic drift did not reduce the overall higher potency of S0*, which included an equally strong
160 humoral response to prototypic spike and VOC Delta (**Fig. 2A, D**).

161 S0*-vaccinated animals were subsequently challenged with each 10^3 $TCID_{50}$ of either of the four VOCs
162 Alpha, Beta, Gamma or Delta, and sacrificed 4 dpi for assessment of viral loads in the lung (**Fig. 2F, G**)
163 and associated lung pathology (**Fig. 2H, I**). In S0*-vaccinated hamsters, viral RNA loads were uniformly

164 reduced compared to matched sham controls by ~3 (VoC Delta) up to ~6 $\log_{10}$ (VoC Gamma) depending
165 on the respective challenge virus under study (**Fig. 2F**). Importantly, no infectious virus could be
166 detected anymore (~6$\log_{10}$ reduction) in any of the animals vaccinated with S0*, irrespective of which
167 VOC they had been exposed to (**Fig. 2G**), confirming 100% VE conferred by S0* against all four VOCs.

168 Protection from infection also translated in a markedly reduced pathology (**Fig. 2H, I**). Non-vaccinated
169 sham animals developed characteristic signs of bronchopneumonia with perivascular and peribronchial
170 infiltrations, edema and consolidation of lung tissues (Abdelnabi et al., 2021; Boudewijns et al., 2020).
171 In contrast, lungs of S0*-vaccinated hamsters remained markedly less affected with a clear reduction in
172 overall histological scores, irrespectively of the VOC used (**Fig. 2H, I**). In conclusion, second-
173 generation YF-S0* expressing an updated S0* antigen induced consistently high levels of broadly
174 neutralizing antibodies (**Fig. 2D**) which translated into efficient protection from lower respiratory tract
175 infection and COVID-19-like pathology by the entire spectrum of circulating VOCs (**Fig. 2G, H**). VE
176 of S0* covered VOC Beta and Gamma, i.e. variants harbouring key mutations K417N/T and E484K
177 escaping original spike-specific nAb activity (**Fig. 2B**), and may therefore offer protection against other
178 emerging variants such as VOI Mu (E484K) with a similar signature.

179 **Blocking of viral transmission**

180 An added benefit of vaccination at the population level would be an efficient reduction in viral shedding
181 and transmission by vaccinated people (Eyre et al., 2021), ideally from single-dose vaccination. For
182 experimental assessment, two groups of hamsters (N=6 each) were either vaccinated once with 10^4 PFU
183 of S0* or sham (Sanchez-Felipe et al., 2021), and were three weeks later intranasally infected with a
184 high dose comprising 10^5 $TCID_{50}$ of VOC Delta to serve as index (donor) animals for direct contact
185 transmission (**Fig. 3A**). At 2 dpi, i.e. at onset of increasing viral loads and shedding (Kaptein et al., 2020;
186 Sia et al. 2020), index animals were each co-housed with one non-vaccinated sentinel for two
187 consecutive days. At 4 dpi, index hamsters were sacrificed, and lungs were assessed for viral RNA,
188 infectious virus and histopathology. Sentinels were sacrificed another two days later and analyzed
189 accordingly.

190 As expected from previous experiments, viral loads in S0*-vaccinated index animals were much lower
191 than in non-vaccinated index animals, or than in sentinels that had been in close contact with non-
192 vaccinated donors (**Fig. 3B, C**). Importantly, only very low levels of viral RNA and no infectious virus
193 was observed in non-vaccinated sentinels that had been co-housed with S0*-vaccinated donors. Also,
194 lung pathology was reduced significantly in vaccinated index and co-housed sentinels as compared to
195 sham vaccinated index and respective co-housed sentinels (**Fig. 3D**). To our knowledge, this is first
196 experimental evidence for full protection from SARS-CoV-2 transmission by any vaccine. The block

197 conferred by S0* appears to be more complete than that observed in humans by current vaccines (Siddle
198 et al., 2021).

199 **Discussion**

200 Little is known about how well current first-generation vaccines protect against the full spectrum of
201 VOCs. While likely protecting from severe COVID-19 caused by any SARS-CoV-2 strain, a clear drop
202 in VE was observed during clinical trials conducted in regions with high circulation of VOC Beta as
203 paradigm of an E484K Spike variant and others known to escape nAb recognition (Sadoff et al., 2021).
204 Experimentally, such a drop in protective immunity is confirmed by higher viral loads in macaques
205 vaccinated with an Adenovirus-vectored prototype spike antigen (Ad26.COV2.S) and challenged with
206 VOC Beta (Yu et al., 2021). Likewise, in the more stringent hamster model, immunity acquired during
207 previous SARS-CoV-2 (prototype) infection, or by Ad26.COV2.S vaccination, led only to partial
208 restraint of heterologous VOC Beta replication (Tostanoski et al.). In the latter case, replicative viral
209 RNA was still detectable two weeks after challenge (< 2 $\log_{10}$ reduction compared to sham), which is
210 completely in line with the observed failure of prototypic YF-S0 to confer full protection against VOC
211 Beta (**Fig. 1F-H**). By contrast, viral replication was reduced to undetectable levels for all four VOCs by
212 YF-S0* vaccination using an updated spike antigen (**Fig. 2G**). Finally, S0* blocked transmission of
213 VOC Delta (**Fig. 3**). In summary, our findings strongly suggest that first-generation COVID-19 vaccines
214 will need to be adapted to keep up with the evolution of variants driving the ongoing global SARS-CoV-
215 2 pandemic, including variants in surge that contain critical combinations of driver mutations
216 responsible for both nAb escape and enhanced transmission. The stringent hamster model is particularly
217 well suited to assess both aspects of preclinical VE, individual protection and transmission (Abdelnabi
218 et al., 2021).

219 Overall combined experimental and abundant clinical evidence suggests that first-generation COVID-
220 19 vaccines employing the prototypic spike (from 2019/early 2020) as antigen may not suffice to cover
221 current circulating and emerging SARS-CoV-2 variants anymore; in particular variants carrying
222 mutations in key epitopes (e.g., those containing K417 and E484) targeted by nAb (Greaney et al., 2021).
223

224 **Methods**

225 **Viruses and animals**

226 All virus-related work was conducted in the high-containment BSL3 facilities of the KU Leuven Rega
227 Institute (3CAPS) under licenses AMV 30112018 SBB 219 2018 0892 and AMV 23102017 SBB 219
228 2017 0589 according to institutional guidelines. All SARS-CoV-2 strains used throughout this study
229 were isolated in house (University Hospital Gasthuisberg, Leuven) and characterized by direct
230 sequencing using a MinION as described before (Boudewijns et al., 2020). Strains representing
231 prototypic SARS-CoV-2 (Wuhan; EPI_ISL_407976) (Boudewijns et al., 2020), VOC Alpha (B.1.117;
232 EPI_ISL_791333) and Beta (B.1.351; EPI_ISL_896474) have been described (Abdelnabi et al., 2021).
233 Strains representing VOC Gamma (P.1; EPI_ISL_1091366) and Delta (B.1.617.2; EPI_ISL_2425097)
234 were local Belgian isolates from March and April 2021, respectively. All virus stocks were grown on
235 Vero E6 cells and used for experimental infections at low *in vitro* passage (P) number, P3 for prototype
236 and P2 for all four VOCs. Absence of furin cleavage site mutations was confirmed by deep sequencing.
237 Median tissue culture infectious doses ($TCID_{50}$) were defined by titration as described (Abdelnabi et al.,
238 2021; Boudewijns et al., 2020) using Vero E6 cells as substrate, except for VOC Delta, for which A549
239 cells were used for a more pronounced virus induced cytopathic effect (CPE).
240 Housing and experimental infections of hamsters have been described (Boudewijns et al., 2020; Kaptein
241 et al., 2020; Sanchez-Felipe et al., 2021) and conducted under supervision of the ethical committee of
242 KU Leuven (license P050/2020 and P055/2021). In brief, 6 to 8 weeks old female Syrian hamsters
243 (*Mesocricetus auratus*) were sourced from Janvier Laboratories and kept per two in individually
244 ventilated isolator cages. Animals were anesthetized with ketamine/xylazine/atropine and intranasally
245 infected with 50 µL of virus stock (25 µL in each nostril) containing either 10^3 or 10^5 $TCID_{50}$ as specified
246 in the text and euthanized 4 days post infection (dpi) for sampling of the lungs and further analysis.
247 Animals were monitored daily for signs of disease (lethargy, heavy breathing, or ruffled fur).
248

249 **Vaccine Candidate**

250 The general methodology for the design and construction of a first YF17D-based SARS-CoV-2 vaccine
251 candidate (YF-S0) has been described (Sanchez-Felipe et al., 2021). Several mutations were introduced
252 into original YF-S0 to generate second-generation vaccine candidate YF-S0*. The first series of
253 mutations is based on the spike sequence of VOC Gamma: L18F, T20N, P26S, D138Y, R190S, K417T,
254 E484K, N501Y, D614G, H655Y, T1027I, V1176F. A second series of mutations is based on a locked
255 spike variant described by Juraszek et al. (2021), stabilizing the protein in a more immunogenic
256 prefusion confirmation: A892P, A942P, V987P (Juraszek et al., 2021).
257

258 **Production of spike-pseudotyped virus and serum neutralization test (SNT)**

259 Virus-neutralizing antibodies (nAb) were determined using a set of VSV spike-pseudotype viruses
260 essentially as described (Sanchez-Felipe et al., 2021). For this purpose, four different pseudotypes were
261 generated using expression plasmids of respective spike variants: for prototype B.1/D614G as before
262 (Sanchez-Felipe et al., 2021) or sourced from Invivogen for VOC Beta (Cat. No. plv-spike-v3), Gamma
263 (Cat. No. plv-spike-v5) and Delta (Cat. No. plv-spike-v8). Briefly, depending on the plasmid
264 background, BHK-21J cells (variant B.1/D614G) or HEK-293T cells (Beta, Gamma and Delta) were
265 transfected with the respective SARS-CoV-2 protein expression plasmids, and one day later infected
266 (MOI = 2) with GFP-encoding VSVΔG backbone virus (Whitt, 2010). Two hours later, the medium was
267 replaced by medium containing anti-VSV-G antibody (I1-hybridoma, ATCC CRL-2700) to neutralize
268 residual VSV-G input. After 24h incubation at 32℃, the supernatants were harvested. To quantify
269 nAb, serial dilutions of serum samples were incubated for 1 hour at 37 °C with an equal volume of S-
270 pseudotyped VSV particles and inoculated on Vero E6 cells for 18 hours.
271 The resulting number of GFP expressing cells was quantified on a Cell Insight CX5/7 High Content
272 Screening platform (Thermo Fischer Scientific) with Thermo Fisher Scientific HCS Studio (v.6.6.0)
273 software. Median serum neutralization titres (SNT_{50}) were determined by curve fitting
274 in Graphpad Prism after normalization to virus (100%) and cell controls (0%) (inhibitor *vs.* response,
275 variable slope, four parameters model with top and bottom constraints of 100% and 0%,
276 respectively).The research reagent for SARS-CoV-2 RNA (NIBSC 20/130) was obtained from the
277 National Institute for Biological Standards and Control, UK (Mattiuzzo et al., 2020).
278
279 **Antigenic cartography**
280 We used the antigenic cartography approach developed for influenza hemagglutination inhibition assay
281 data to study the antigenic characteristics of the SARS-CoV-2 Spikes (Smith et al., 2004). This approach
282 transforms SNT_{50} data to a matrix of immunological distances. Immunological distance d_{ij} is defined as
283 $d_{ij} = s_j - H_{ij}$, where H_{ij} is the $\log_2$ titre of virus i against serum j and s_j is the maximum observed titre to
284 the antiserum from any antigen ($s_j = \max(H_{1j}, \ldots, H_{nj})$). Subsequently, a multidimensional scaling
285 algorithm was used to position points representing antisera and antigens in a two-dimensional space
286 such that their distances best fit their respective immunological distances. Even though distances are
287 measured between sera raised by vaccination using specific Spike antigens (and the pooled NIBSC
288 serum) and antigens, such an antigenic map also provides estimates of antigenic distances between the
289 antigens themselves.
290
291 **Vaccination and challenge**
292 COVID-19 vaccine candidate YF-S0 (Sanchez-Felipe et al., 2021) was used to vaccinate hamsters at
293 day 0 and day 7 (N=32) with a dose of 10^4 PFU via the intraperitoneal route and control animals (N=18)
294 were dosed with MEM (Modified Earl's Minimal) medium containing 2% bovine serum as sham
295 controls. Blood was drawn at day 21 for serological analysis and infection was done on the same day

296 with prototype (N=10 vaccinated; N=6 sham), VOC Alpha (N=10 vaccinated; and N=6 sham), and Beta
297 variant (N=12 vaccinated; N=6 sham) with the inoculum of 10^3 $TCID_{50}$ intranasally. Protective nAb
298 levels were calculated using logistic regression analysis in GraphPad Prism (version 9) as described (van
299 der Lubbe et al., 2021)

300 Similarly, hamsters were vaccinated twice with 10^4 YF-S0* (N=24) or sham (N=16) at day 0 and day 7.
301 Blood was collected at day 21 to analyze nAb in serum, and animals were infected on day 24 with
302 different variants, including VOC Alpha, Beta, Gamma and Delta with the inoculum of 10^3 TCID50
303 intranasally (N=6 vaccinated and N=4 sham vaccinated infected against each variant). Lungs were
304 collected for analysis of viral RNA, infectious virus and for histopathological examination as described
305 in (Sanchez-Felipe et al., 2021). Resulting vaccine efficacy (VE) was calculated as [1 – (number of
306 vaccinated animals with detectable virus) / (number of all infected animals)] x 100% per group of
307 hamsters infected with the same virus strain, whereby a lung viral load $>10^2$ $TCID_{50}$/100mg was set as
308 cutoff for infection (van der Lubbe et al., 2021).

309 **Viral load and viral RNA quantification**
310 Virus loads were determined by titration and RT-qPCR from lung homogenates was performed exactly
311 as previously described in detail (Boudewijns et al., 2020; Kaptein et al., 2020; Sanchez-Felipe et al.,
312 2021).
313
314 **Histopathology**
315 For histological examination, the lungs were fixed overnight in 4% formaldehyde, embedded in paraffin
316 and tissue sections (5 µm) after staining with H&E scored blindly for lung damage (cumulative score of
317 1 to 3 each for congestion, intra-alveolar hemorrhage, apoptotic bodies in bronchial epithelium,
318 necrotizing bronchiolitis, perivascular edema, bronchopneumonia, perivascular inflammation,
319 peribronchial inflammation, and vasculitis) as previously established (Abdelnabi et al., 2021;
320 Boudewijns et al., 2020)
321
322 **Blocking of viral transmission**
323 Hamsters (N=6) were vaccinated with 10^4 PFU of vaccine once, were bled at day 21 and infected with
324 delta variant with $1x10^5$ TCID50, intranasally. Another group of non-vaccinated hamsters (N=6) were
325 also infected. Two days post infection index animals were co-housed with sentinels for two days and
326 separated after two days of exposure. All the index animals were euthanized on day four post infection
327 and sentinels were sacrificed after 4 days of exposure. Lungs were analyzed for viral RNA and infectious
328 virus and subjected to histopathology.
329
330 **Statistical analysis**

331 All statistical analyses were performed using GraphPad Prism 9 software (GraphPad, San Diego, CA,
332 USA). Results are presented as GM± IQR or medians ± IQR as indicated. Data were analyzed using
333 uncorrected Kruskal-Wallis test and considered statistically significant at p-values ≤0.05.
334

335 **Acknowledgements**

336 We are grateful to Prof. Michael A. Whitt (University of Tennessee Health Science Center) for
337 generously sharing of plasmids for rescue of VSVΔG, and Dr. Maya Imbrechts and Dr. Nick Geukens
338 (PharmAbs, KU Leuven) for help with hybridoma culture. We thank Carolien De Keyzer and Lindsey
339 Bervoets (Rega) for excellent technical assistance with animal experimentation as well as the staff of
340 the Rega animalium for strong support. We thank Jasper Rymenants, Tina van Buyten, Dagmar Buyst
341 and Thibault Francken for steady and timely help with analysing of tissue samples and virus titrations.
342 We finally thank Jasmine Paulissen, Madina Rasulova, Catherina Coun and Nathalie Thys (TPVC) for
343 diligent serology assessment and skilled generation of plasmid constructs.
344

345 Current work was supported by the Flemish Research Foundation (FWO) emergency COVID-19 fund
346 (G0G4820N) and the FWO Excellence of Science (EOS) program (No. 30981113; VirEOS project), the
347 European Union's Horizon 2020 research and innovation program (No 101003627; SCORE project and
348 No 733176; RABYD-VAX consortium), the Bill and Melinda Gates Foundation (INV-00636), KU
349 Leuven Internal Funds (C24/17/061) and the KU Leuven/UZ Leuven Covid-19 Fund (COVAX-PREC
350 project). G.B. acknowledges support from the KU Leuven Internal Funds (Grant No. C14/18/094) and
351 the Research Foundation - Flanders ("Fonds voor Wetenschappelijk Onderzoek - Vlaanderen,"
352 G0E1420N, G098321N). P.L. acknowledges funding from the European Research Council under the
353 European Union's Horizon 2020 research and innovation program (grant agreement no. 725422-
354 ReservoirDOCS). K.D. acknowledges grant support from KU Leuven Internal Funds (C3/19/057 Lab
355 of Excellence).
356

357 **Contributions**

358 S.S. and K.D. conceptualization; S.S. animal experimentation; S.S., T.V., W.K. and H.J.T. data
359 generation, analysis and curation; S.S. and K.D. original manuscript draft; S.S. and H.J.T. visualization;
360 T.V. and L.S.F. construct design; T.V., W.K. and D.V.L. serological analysis; R.A. and C.S.F. VoC
361 hamster models; B.W. histological analysis; P.L. and G.B. antigenic cartography; L.S.F., V.L. and P.M.
362 vaccine stocks and virus isolation; J.N., H.J.T., and K.D. supervision, writing and project administration;
363 J.N. and K.D. funding acquisition. All authors read, edited and approved the final version of the
364 manuscript.
365

366 **References**

367

368 Abdelnabi, R., Boudewijns, R., Foo, C.S., Seldeslachts, L., Sanchez-Felipe, L., Zhang, X., Delang,
369 L., Maes, P., Kaptein, S.J.F., Weynand, B.*, et al.* (2021). Comparing infectivity and virulence of
370 emerging SARS-CoV-2 variants in Syrian hamsters. EBioMedicine *68*, 103403.

371 Boudewijns, R., Thibaut, H.J., Kaptein, S.J.F., Li, R., Vergote, V., Seldeslachts, L., Van
372 Weyenbergh, J., De Keyzer, C., Bervoets, L., Sharma, S.*, et al.* (2020). STAT2 signaling restricts
373 viral dissemination but drives severe pneumonia in SARS-CoV-2 infected hamsters. Nat
374 Commun *11*, 5838.

375 Cella, E., Benedetti, F., Fabris, S., Borsetti, A., Pezzuto, A., Ciotti, M., Pascarella, S., Ceccarelli,
376 G., Zella, D., Ciccozzi, M.*, et al.* (2021). SARS-CoV-2 Lineages and Sub-Lineages Circulating
377 Worldwide: A Dynamic Overview. Chemotherapy *66*, 3-7.

378 Cherian, S., Potdar, V., Jadhav, S., Yadav, P., Gupta, N., Das, M., Rakshit, P., Singh, S., Abraham,
379 P., Panda, S.*, et al.* (2021). Convergent evolution of SARS-CoV-2 mutations, L452R, E484Q and
380 P681R, in the second wave of COVID-19 in Maharashtra, India. bioRxiv,
381 2021.2004.2022.440932.

382 Collier, D.A., De Marco, A., Ferreira, I., Meng, B., Datir, R.P., Walls, A.C., Kemp, S.A., Bassi, J.,
383 Pinto, D., Silacci-Fregni, C.*, et al.* (2021). Sensitivity of SARS-CoV-2 B.1.1.7 to mRNA vaccine-
384 elicited antibodies. Nature *593*, 136-141.

385 ECDC (2021). SARS-CoV-2 variants of concern as of 7 October 2021.

386 Eyre, D.W., Taylor, D., Purver, M., Chapman, D., Fowler, T., Pouwels, K.B., Walker, A.S., and
387 Peto, T.E. (2021). The impact of SARS-CoV-2 vaccination on Alpha & Delta variant transmission.
388 medRxiv, 2021.2009.2028.21264260.

389 Graham, M.S., Sudre, C.H., May, A., Antonelli, M., Murray, B., Varsavsky, T., Kläser, K., Canas,
390 L.S., Molteni, E., Modat, M.*, et al.* (2021). Changes in symptomatology, reinfection, and
391 transmissibility associated with the SARS-CoV-2 variant B.1.1.7: an ecological study. Lancet
392 Public Health *6*, e335-e345.

393 Greaney, A.J., Loes, A.N., Crawford, K.H.D., Starr, T.N., Malone, K.D., Chu, H.Y., and Bloom, J.D.
394 (2021). Comprehensive mapping of mutations in the SARS-CoV-2 receptor-binding domain
395 that affect recognition by polyclonal human plasma antibodies. Cell Host Microbe *29*, 463-
396 476.e466.

397 Hoffmann, M., Arora, P., Groß, R., Seidel, A., Hörnich, B.F., Hahn, A.S., Krüger, N., Graichen, L.,
398 Hofmann-Winkler, H., Kempf, A.*, et al.* (2021). SARS-CoV-2 variants B.1.351 and P.1 escape
399 from neutralizing antibodies. Cell *184*, 2384-2393.e2312.

400 Holmes, E.C., Goldstein, S.A., Rasmussen, A.L., Robertson, D.L., Crits-Christoph, A., Wertheim,
401 J.O., Anthony, S.J., Barclay, W.S., Boni, M.F., Doherty, P.C.*, et al.* (2021). The origins of SARS-
402 CoV-2: A critical review. Cell *184*, 4848-4856.

403 Hsieh, C.L., Goldsmith, J.A., Schaub, J.M., DiVenere, A.M., Kuo, H.C., Javanmardi, K., Le, K.C.,
404 Wrapp, D., Lee, A.G., Liu, Y.*, et al.* (2020). Structure-based design of prefusion-stabilized SARS-
405 CoV-2 spikes Science *369*, 1501-1505.

406 Juraszek, J., Rutten, L., Blokland, S., Bouchier, P., Voorzaat, R., Ritschel, T., Bakkers, M.J.G.,
407 Renault, L.L.R., and Langedijk, J.P.M. (2021). Stabilizing the closed SARS-CoV-2 spike trimer.
408 Nat Commun *12*, 244.

409 Kaptein, S.J.F., Jacobs, S., Langendries, L., Seldeslachts, L., Ter Horst, S., Liesenborghs, L., Hens,
410 B., Vergote, V., Heylen, E., Barthelemy, K.*, et al.* (2020). Favipiravir at high doses has potent
411 antiviral activity in SARS-CoV-2-infected hamsters, whereas hydroxychloroquine lacks activity.
412 Proc Natl Acad Sci U S A *117*, 26955-26965.

413 Kyriakidis, N.C., López-Cortés, A., González, E.V., Grimaldos, A.B., and Prado, E.O. (2021).
414 SARS-CoV-2 vaccines strategies: a comprehensive review of phase 3 candidates. NPJ Vaccines
415 *6*, 28.

416 Liu, J., Liu, Y., Xia, H., Zou, J., Weaver, S.C., Swanson, K.A., Cai, H., Cutler, M., Cooper, D., Muik,
417 A.*, et al.* (2021a). BNT162b2-elicited neutralization of B.1.617 and other SARS-CoV-2 variants.
418 Nature *596*, 273-275.

419 Liu, Y., Liu, J., Johnson, B.A., Xia, H., Ku, Z., Schindewolf, C., Widen, S.G., An, Z., Weaver, S.C.,
420 Menachery, V.D.*, et al.* (2021b). Delta spike P681R mutation enhances SARS-CoV-2 fitness over
421 Alpha variant. bioRxiv.

422 Lopez Bernal, J., Andrews, N., Gower, C., Gallagher, E., Simmons, R., Thelwall, S., Stowe, J.,
423 Tessier, E., Groves, N., Dabrera, G.*, et al.* (2021). Effectiveness of Covid-19 Vaccines against
424 the B.1.617.2 (Delta) Variant. N Engl J Med *385*, 585-594.

425 Madhi, S.A., Baillie, V., Cutland, C.L., Voysey, M., Koen, A.L., Fairlie, L., Padayachee, S.D.,
426 Dheda, K., Barnabas, S.L., Bhorat, Q.E.*, et al.* (2021). Efficacy of the ChAdOx1 nCoV-19 Covid-
427 19 Vaccine against the B.1.351 Variant. N Engl J Med *384*, 1885-1898.

428 Martin, D.P., Weaver, S., Tegally, H., San, J.E., Shank, S.D., Wilkinson, E., Lucaci, A.G.,
429 Giandhari, J., Naidoo, S., Pillay, Y.*, et al.* (2021). The emergence and ongoing convergent
430 evolution of the SARS-CoV-2 N501Y lineages. Cell *184*, 5189-5200.e5187.

431 Mattiuzzo, G., Bentley, E.M., Hassall, M., Routley, S., Richardson, S., Bernasconi, V.,
432 Kristiansen, P., Harvala, H. , Roberts, D., Semple, M.G., Turtle, L.C.W., Openshaw P.J.M., *et al.*
433 (2020). Establishment of the WHO International Standard and Reference Panel for anti-SARS-
434 CoV-2antibody. WHO/BS/2020.2403.

435 Moyo-Gwete, T., Madzivhandila, M., Makhado, Z., Ayres, F., Mhlanga, D., Oosthuysen, B.,
436 Lambson, B.E., Kgagudi, P., Tegally, H., Iranzadeh, A.*, et al.* (2021). SARS-CoV-2 501Y.V2
437 (B.1.351) elicits cross-reactive neutralizing antibodies. bioRxiv, 2021.2003.2006.434193.

438 Muik, A., Wallisch, A.K., Sänger, B., Swanson, K.A., Mühl, J., Chen, W., Cai, H., Maurus, D.,
439 Sarkar, R., Türeci, Ö.*, et al.* (2021). Neutralization of SARS-CoV-2 lineage B.1.1.7 pseudovirus
440 by BNT162b2 vaccine-elicited human sera. Science *371*, 1152-1153.

441 Rubin, R. (2021). COVID-19 Vaccines vs Variants-Determining How Much Immunity Is Enough.
442 Jama *325*, 1241-1243.

443 Sabino, E.C., Buss, L.F., Carvalho, M.P.S., Prete, C.A., Jr., Crispim, M.A.E., Fraiji, N.A., Pereira,
444 R.H.M., Parag, K.V., da Silva Peixoto, P., Kraemer, M.U.G.*, et al.* (2021). Resurgence of COVID-
445 19 in Manaus, Brazil, despite high seroprevalence. Lancet *397*, 452-455.

446 Sadoff, J., Gray, G., Vandebosch, A., Cárdenas, V., Shukarev, G., Grinsztejn, B., Goepfert, P.A.,
447 Truyers, C., Fennema, H., Spiessens, B.*, et al.* (2021). Safety and Efficacy of Single-Dose
448 Ad26.COV2.S Vaccine against Covid-19. N Engl J Med *384*, 2187-2201.

449 Sanchez-Felipe, L., Vercruysse, T., Sharma, S., Ma, J., Lemmens, V., Van Looveren, D.,
450 Arkalagud Javarappa, M.P., Boudewijns, R., Malengier-Devlies, B., Liesenborghs, L.*, et al.*
451 (2021). A single-dose live-attenuated YF17D-vectored SARS-CoV-2 vaccine candidate. Nature
452 *590*, 320-325.

453 Siddle, K.J., Krasilnikova, L.A., Moreno, G.K., Schaffner, S.F., Vostok, J., Fitzgerald, N.A.,
454 Lemieux, J.E., Barkas, N., Loreth, C., Specht, I.*, et al.* (2021). Evidence of transmission from fully
455 vaccinated individuals in a large outbreak of the SARS-CoV-2 Delta variant in Provincetown,
456 Massachusetts. medRxiv.

457 Smith, D.J., Lapedes, A.S., de Jong, J.C., Bestebroer, T.M., Rimmelzwaan, G.F., Osterhaus, A.D.,
458 and Fouchier, R.A. (2004). Mapping the antigenic and genetic evolution of influenza virus.
459 Science *305*, 371-376.

460 Tian, D., Sun, Y., Zhou, J., and Ye, Q. (2021). The global epidemic of SARS-CoV-2 variants and
461 their mutational immune escape. J Med Virol. 2021 Oct 5. doi: 10.1002/jmv.27376.

462 Tostanoski, L.H., Yu, J., Mercado, N.B., McMahan, K., Jacob-Dolan, C., Martinot, A.J., Piedra-
463 Mora, C., Anioke, T., Chang, A., Giffin, V.M.*, et al.* Immunity elicited by natural infection or
464 Ad26.COV2.S vaccination protects hamsters against SARS-CoV-2 variants of concern. Science
465 Translational Medicine *0*, eabj3789.

466 van der Lubbe, J.E.M., Rosendahl Huber, S.K., Vijayan, A., Dekking, L., van Huizen, E.,
467 Vreugdenhil, J., Choi, Y., Baert, M.R.M., Feddes-de Boer, K., Izquierdo Gil, A.*, et al.* (2021).
468 Ad26.COV2.S protects Syrian hamsters against G614 variant SARS-CoV-2 and does not
469 enhance respiratory disease. NPJ Vaccines *6*, 39.

470 Wang, P., Nair, M.S., Liu, L., Iketani, S., Luo, Y., Guo, Y., Wang, M., Yu, J., Zhang, B., Kwong,
471 P.D.*, et al.* (2021). Antibody resistance of SARS-CoV-2 variants B.1.351 and B.1.1.7. Nature *593*,
472 130-135.

473 Whitt, M.A. (2010). Generation of VSV pseudotypes using recombinant ΔG-VSV for studies on
474 virus entry, identification of entry inhibitors, and immune responses to vaccines. J Virol
475 Methods *169*, 365-374.

476 Wu, K., Werner, A.P., Moliva, J.I., Koch, M., Choi, A., Stewart-Jones, G.B.E., Bennett, H.,
477 Boyoglu-Barnum, S., Shi, W., Graham, B.S.*, et al.* (2021). mRNA-1273 vaccine induces
478 neutralizing antibodies against mutants from global SARS-CoV-2 variants. bioRxiv,
479 2021.2001.2025.427948.

480 Yadav, P.D., Sapkal, G.N., Abraham, P., Ella, R., Deshpande, G., Patil, D.Y., Nyayanit, D.A.,
481 Gupta, N., Sahay, R.R., Shete, A.M.*, et al.* (2021). Neutralization of variant under investigation
482 B.1.617 with sera of BBV152 vaccinees. Clin Infect Dis.

483 Yu, J., Tostanoski, L.H., Mercado, N.B., McMahan, K., Liu, J., Jacob-Dolan, C., Chandrashekar,
484 A., Atyeo, C., Martinez, D.R., Anioke, T.*, et al.* (2021). Protective efficacy of Ad26.COV2.S
485 against SARS-CoV-2 B.1.351 in macaques. Nature *596*, 423-427.

486

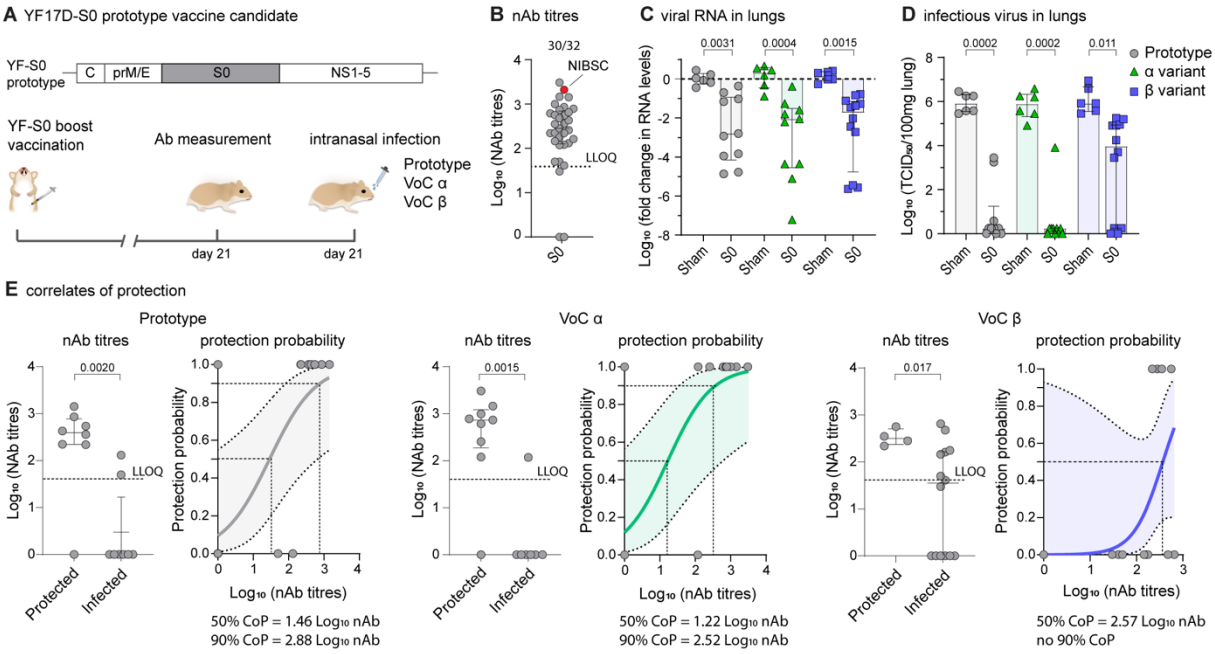

Figure 1. Immunogenicity and protective efficacy of first-generation Spike vaccine against VOCs Alpha and Beta. A, Vaccination scheme with prototypic YF17D-based vaccine candidate YF-S0 (S0). Syrian hamsters were immunized twice intraperitoneally with 10^4 PFU of S0 on day 0 and 7 and inoculated intranasally on day 21 with 10^3 median tissue-culture infectious dose ($TCID_{50}$) of either prototype SARS-CoV-2 (*grey circles*), VOC Alpha (*green triangles*) or VOC Beta (*blue squares*). **B**, nAb titers against prototypic spike (D614G) pseudotyped virus on day 21 after vaccination. Red datapoint indicates the NIBSC 20/130 human reference sample included as benchmark. **C, D**, Viral loads in hamster lungs four days after infection quantified by quantitative RT-PCR (**C**) and virus titration (**D**). **E**, correlates of protection against prototype SARS-CoV-2, VOC Alpha and VOC Beta. Logistic regression model to calculate nAb titers correlating with 50% and 90% probability for protection. '*Protected'* was defined by a viral load <10^2 $TCID_{50}$/100mg lung tissue and '*infected'* by a viral load >10^2 $TCID_{50}$/100mg lung tissue (van der Lubben et al., 2021). Shaded areas indicate 95% CI. LLOQ is lower limit of quantification. Error bars denote median ± IQR. Data were analyzed using uncorrected Kruskal-Wallis.

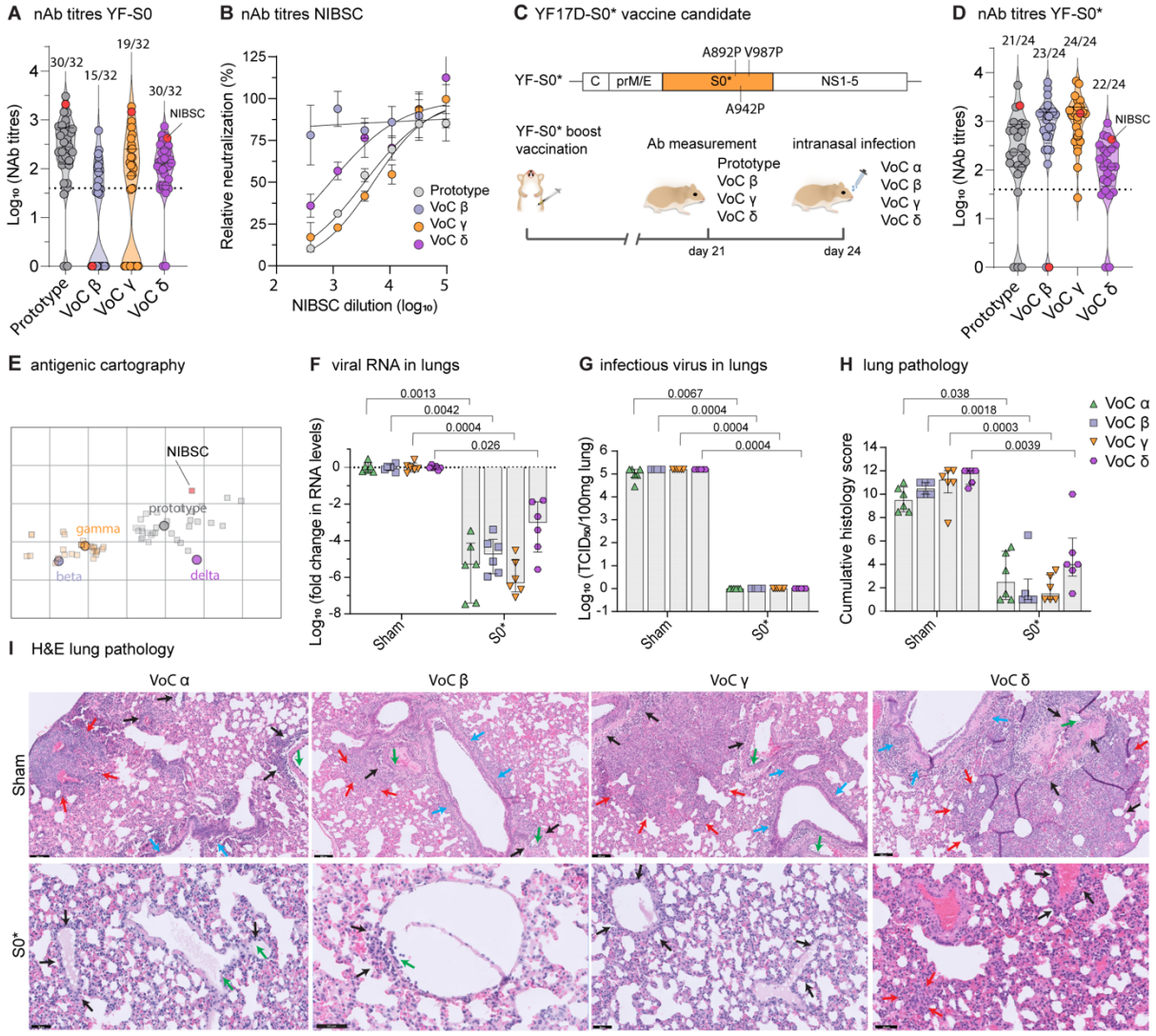

Figure 2. A vaccine based on the updated Spike antigen S0* offers complete protection against all four VOCs. A, nAb titers against prototypic (*grey*), VOC Beta (*blue*), VOC Gamma (*orange*) and VOC Delta (*purple*) spike pseudotyped virus on day 21 after vaccination with prototype YF-S0. Red datapoint indicates the NIBSC 20/130 human reference sample (see Fig. 1B). **B**, Neutralization curves for NIBSC 20/130 human reference sample against same set of pseudotyped viruses. **C**, Schematic of the updated YF-S0* (S0*) vaccine candidate based on VOC Gamma, plus three extra stabilizing proline residues. Vaccination scheme with YF-S0*. Syrian hamsters were immunized twice intraperitoneally with 10^4 PFU of S0* on day 0 and 7 and inoculated intranasally on day 24 with 10^3 median tissue-culture infectious dose ($TCID_{50}$) of either VOC Alpha (*green*), VOC Beta (*blue*), VOC Gamma (*orange*) and VOC Delta (*purple*). **D**, nAb titers against prototypic, VOC Beta, VOC Gamma and VOC Delta spike pseudotyped virus on day 21 after vaccination with YF-S0*. Red datapoint indicates the NIBSC 20/130 human reference sample. **E**, antigenic cartography. Cross-reactivity of the sera raised by original S0 (*grey squares*) and updated S0* (*orange squares*) vaccine antigen against four different virus variants (circles: prototype, *grey*; VOC Beta, *blue*; Gamma, *orange*, and Delta, *purple*) plotted on two-dimensional distance map (Smith et al., 2004). **F, G,** Viral loads in hamster lungs four days after infection quantified by quantitative PCR with reverse transcription (RT–qPCR) (**F**) and virus titration (**G**). **H**, cumulative lung pathology scores from H&E-stained slides of lungs for signs of damage. **I**, Representative H&E-stained images of sham- or S0*-vaccinated hamster lungs after challenge. Perivascular inflammation (*black arrows*) with focal endothelialitis (*green arrows*); peri-bronchial inflammation (*blue arrows*); patches of bronchopneumonia (*red arrows*). Error bars denote median ± IQR. Data were analyzed using uncorrected Kruskal-Wallis.

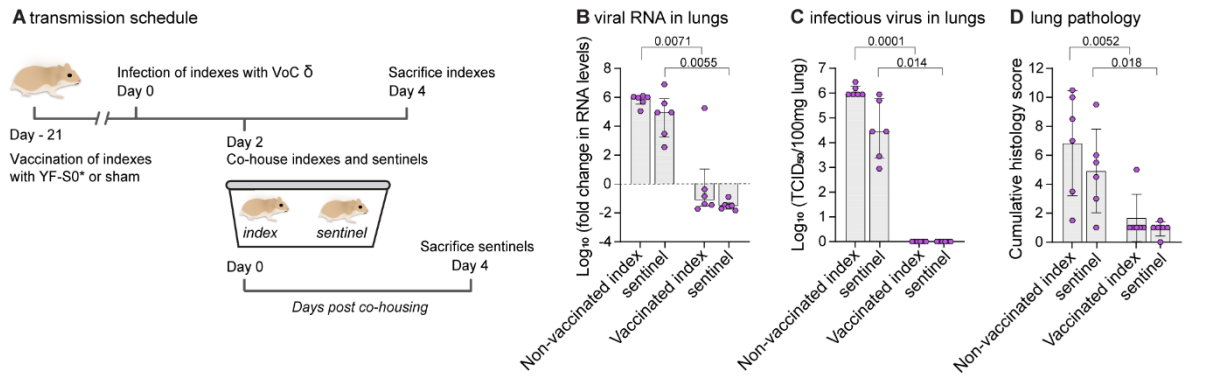

Figure 3. A vaccine based on the updated Spike antigen S* completely prevents transmission of the Delta variant. Effect of YF-S0* vaccination on viral transmission to non-vaccinated contact hamsters. Index hamsters were either sham-vaccinated or vaccinated with a single dose of 10^4 PFU of YF-S0* and infected intranasally on day 21 with 10^5 $TCID_{50}$ of VOC Delta. Two days after infection, index animals were paired and co-housed with each one naïve sentinel. Index and sentinel animals were sacrificed each 4 days after infection or exposure, respectively. **B, C,** Viral loads in hamster lungs four days after infection quantified by quantitative RT-qPCR (**B**) and virus titration (**C**). **D**, cumulative lung pathology scores from H&E-stained slides of lungs for signs of damage. Error bars denote median ± IQR. Data were analyzed using uncorrected Kruskal-Wallis.